Canadian Journal of Physics
Revue canadienne de physique

SYNTHESIS, STRUCTURE AND ELECTRICAL PROPERTIES OF MOLYBDENUM DISULFIDE / MESOPOROUS CARBON NANOCOMPOSITE

SCHOLARONE™
Manuscripts

SYNTHESIS, STRUCTURE AND ELECTRICAL PROPERTIES OF MOLYBDENUM DISULFIDE / MESOPOROUS CARBON NANOCOMPOSITE

Lyudmyla Shyyko*, Volodymyr Kotsyubynsky, Ivan Budzulyak, Ivan Yaremiy, Bogdan Rachiy

Department of Materials science and new technology, Vasyl Stefanyk Precarpathian National University, 57 Shevchenko str., 76018 Ivano-Frankivsk, Ukraine

*Corresponding author, email: lyudmylas13@gmail.com, phone: +380673436942

ABSTRACT

Mesoporous carbon, received from a raw material of plant origin and activated with orthophosphoric acid was used as a good supplement for molybdenum disulfide for creation a nanocomposite with improved electrical properties. Synthesized via hydrothermal method using cetyltrimethylammonium cations the composite was characterised by X-ray diffractometry (XRD), Transmission electron microscopy (TEM), Small angle X-ray scattering (SAXS), porosimetry and impedance spectroscopy. Obtained material has a structure of multilayer sheets dispersed in amorphous carbon filling its pores and poses electric conductivity three times higher than of single mesoporous carbon and almost thirteen times than of the commercial MoS_2 (0.51 $mS \cdot m^{-1}$, 0.18 $mS \cdot m^{-1}$ and 0.038 $mS \cdot m^{-1}$ respectively). Additionaly, the samples were annealed in Ar atmospehere at $500^{\circ}C$ for 2 hours, but it had not significant effect on composite structure, that indicating the temperature stability of the material.

RÉSUMÉ

Mesoporous carbone, reçu d'une matière première d'origine végétale et activé avec de l'acide orthophosphorique a été utilisé comme un bon complément pour le disulfure de molybdène, pour la création d'un nanocomposite avec des propriétés électriques améliorées. Synthétisé par voie hydrothermale utilisant des cations cetyltrimethylammonium le composite a été caractérisé par diffractométrie de rayons X (XRD), microscopie électronique en transmission (MET), diffusion des rayons X aux petits angles (SAXS), porosimétrie et spectroscopie d'impédance. Le matériau obtenu

a une structure de feuilles multicouches dispersées dans du carbone amorphe remplissant ses pores et pose une conductivité électrique trois fois plus élevée que du simple carbone mésoporeux et près de treize fois plus que de l'MoS$_2$ commerciale (respectivement, 0.51 mS·m^{-1}, 0.18 mS·m^{-1} and 0.038 mS·m^{-1}). De plus, les échantillons ont été recuit dans de l'atmosphère d'Argone à 500°C pendant 2 heures, mais il a eu un effet non significatif sur la structure du composite, ce qui indique la stabilité de la température de la matière.

Keywords: molybdenum disulfide, mesoporous carbon, hydrothermal synthesis, nanocomposite, electrical conductivity

1. INTRODUCTION

The rapid development of chemical power sources and the need to improve their operating parameters stimulate researchers to study different materials that may be used as a cathode - active matrix paired with lithium or lithium containing anode. It is widely known, that a magnitude and type of conductivity of the material, as well as its structure, significantly affect the implementation processes of lithium [1]. In the best case host material must have sufficient both electronic and ionic conductivity and be abble to revercibly intercalate-deintercalate Li ions. Porous carbon materials are widely used in separation, catalysis and energy storage and generation. However, its application in high-energy Li-ion batteries (LIBs) is largely hampered by the relatively low theoretical capacity (for graphite it is 372 mAhg^{-1}). Regarding molybdenum disulfide (MoS_2), which belongs to layered transition-metal dichalcogenides, as an electrode material for the same purpose, the feature of MoS_2 layered structure allows the Li+ ions to diffuse without significant increase in volume. Despite its specific capacity is much higher than for graphite (approximately 700 mAhg^{-1}), there is still an effort of low ion/electron conductivity. According to latest tendencies the composite structure based on MoS_2 and carbonaceous matrix materials solved this problem and is highly promising as high-performance electrodes for LIBs. In addition, the feature of MoS_2 is the ability to form structures with different morphology and size, affecting the properties of this material. In particular, the flower-like particles [2], nanospheres [3], nanorods [4] and single layers [5] have been already synthesized. However, as in the most of nanoscale materials, there are the problems of aggregation and restacking during the repetitive cycling and even the drying process of electrodes, not forgetting also that MoS_2 is a semiconductor with a very low conductivity. All these issues would result in the loss of the unusual properties of the graphene-like MoS_2 and the negative effects on their properties. If the graphene-like MoS_2 nanosheets are uniformly dispersed in other medium such as carbon material, their aggregation will be effectively inhibited, which leads to enhanced electrochemical properties. The amorphous carbon can stabilize the disordered structure of the MoS_2 nanoparticles throughout the cycling regime to accommodate more Li$^+$ ions, and also keep the active materials electrically connected [6, 7].

We have investigated the possibility of obtaining the nanocomposite MoS_2 / C with high conductivity for high-energy electrochemical devices such as Li-ion batteries (LIBs). Here we present simple synthesis method of molybdenum disulfide / mesoporous carbon nanocomposite, that does not require significant energy, is low-cost and environmentally friendly. In addition we compare the electric conductivity of commercial MoS_2 (Merck, Germany), mesoporous carbon obtained from raw material of plant origin and synthesized molybdenum disulfide / mesoporous carbon nanocomposite.

2. MATERIALS AND METHODS

2.1. Materials preparation

2.1.1. Mesoporous carbon preparation

The powder of ground apricot seeds was used as the raw material for mesoporous carbon. 50 g of apricot seeds powder was mixed with 400 ml 30% H_3PO_4 and left for 1 h, after the mixture was thermally treated at the temperature of 550^oC on air for 1 hour with the further annealing in Ar atmosphere at 500^oC for 2 hours.

2.1.2. Precursor preparation

Molybdate ammonium $(NH_4)_2MoS_4$ was a precursor for MoS_2 synthesis, which was pre-prepared by following procedure: 5.88 g of $(NH_4)_2MoO_4$ was dissolved in 40.8 ml of 20% $(NH_4)_2S$. After stirring during 30 minutes at the room temperature the dark yellow precipitate of $(NH_4)_2MoS_4$ was formed (Eq.1):
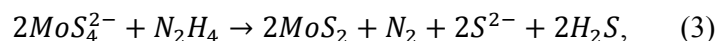
$$(NH_4)_2MoO_4 + 4(NH_4)_2S \rightarrow (NH_4)_2MoS_4 + 8NH_4 \cdot OH \qquad (1)$$
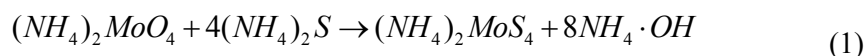
2.1.3. Synthesis of MoS₂/C nanocomposite

Resulting $(NH_4)_2MoS_4$ was mixed with 1.98 ml of hydrazine hydrate $N_2H_4 \cdot N_2O$ and 100 ml of distilled water. The pH level of the reaction medium was 7.6 and regulated by HCl. After adding

1 g of cetyltrimethylammonium bromide $C_{19}H_{42}BrN$ and 1 g of mesoporous carbon the solution was put into Teflon autoclave and stored at the temperature of 220^oC for 24 hours.

Chemical reactions that took place in hydrothermal synthesis are (Eq. 2, 3) [24]:

$$2\left(NH_4\right)_2 MoS_4 + N_2H_4 \rightarrow 2MoS_2 + 4H_2S + 4NH_3 + N_2, \qquad (2)$$

$$2MoS_4^{2-} + N_2H_4 \rightarrow 2MoS_2 + N_2 + 2S^{2-} + 2H_2S, \qquad (3)$$
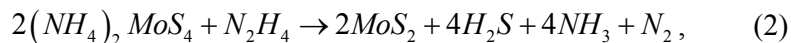
The resulting black precipitate was washed with distilled water and ethanol, and after centrifugation dried at 80^oC. Additionally, the obtained material was annealed in argon atmosphere at 500^oC for 2 hours.

2.2. Materials characterization

The synthesized material phase composition and structure were investigated by XRD and SAXS methods (DRON-3 diffractometer, Cu K_α radiation). Morphological characteristics and chemical composition were obtained by TEM and EDS (FEI Technai G2 X-TWIN microscope). The specific surface area and pore size distribution were measured by nitrogen adsorption at 77.2 K (Quantachrome NOVA 2200e porosimeter). Electrical conductivity σ as a function of frequency was measured by the method of impedance spectroscopy in the frequency range of $0.01 - 100$ kHz (Autolab PGSTAT 12/FRA-2 analyser), all samples were made in pellet form with the diameter of $17 \cdot 10^{-3}$ m and thikness of $0.1 \cdot 10^{-3}$ m under pressure of 34 MPa at room temperature.

3. RESULTS

According to XRD the synthesized material is nearly to X-ray amorphous, however there are two areas of increased intensity of diffracted X-rays: in the angle 2θ about 33.4^o and 58.2^o and can be associated with (100) and (110) reflections of $2H$-MoS_2 crystal structure, which belongs to hexagonal system and P63/mmc symetry group (Fig. 1, a). The (002) peak in the vicinity of $2\theta = 14$-

15° typical for this structure was not indentified. It, according to [8-10], indicates the lack of connection between the individual MoS_2 layers and the formation of graphene-like structure.

After annealing in Ar atmosphere at $500^{\circ}C$ during 2 hours, the reflection corresponding to the family of (110) planes, has shifted to higher angles by 2.2°, while the chage in (100) reflection position is within acceptable error (Fig. 1, b). This fact shows the change of interatomic distances within (001) plane, i.e. along the layers formed by Mo atoms placed between two layers of S atoms, forming a trigonal prism. But in general it can be concluded that annealing did not significantly affect the morphology and composition of the nanocomposite.

TEM images (Fig. 2) show, that synthesized nanocomposite consists of stacked nanosheets (7-9) of MoS_2 characterized by crystalline order and dispersed in amorphous carbon (Fig. 2 a, b, c). According to EDS analysis the relative content of carbon atoms along 2 μm line (Fig. 2 d) is at least 35 at.% (Fig.3). Concentrations of Mo, S and O in the sample along 2 μm line are also shown in Fig.3.

The results of nitrogen sorption, in particular, the pore size distribution of mesoporous carbon and synthesized nanocomposite (Fig. 4), confirmed that nanoparticles of molybdenum disulfide have localized in micro and mesopores of carbon material. Comparing the pore size distributions of carbon and nanocomposite (black and gray colors in Fig.4), one can see the difference in the pore width range of 0-8 nm. The surface areas, calculated by the BET method from nitrogen sorption curves, of mesoporous carbon and MoS_2/C nanocomposite are 2200 $m^2 \cdot g^{-1}$ and 430 $m^2 \cdot g^{-1}$, respectively.

More information on the internal microstructure of the synthesized material we have obtained through the method of small-angle X-ray scattering (Fig. 5). Scattering intensity curves of the samples are presented in double logarithmic coordinates. The volumetric distribution function of inhomogeneities was calculated using GNOM (Institute of Crystallography RAS, Moscow) in the model of homogeneous polydisperse spheres [11].

As seen from the data scattering intensity curves of both samples show a similar character. The curves can be devided into three angular regions of $I(s)$ dependance (I is the scattering intesity, s is the module of the wave vector and $s = \dfrac{4\pi}{\lambda}\sin(\theta)$, 2θ is the scattering angle). In the (s_{min}, s_1) range the scattering intensity is described by Guinier's law and corresponds to the scattering of X-rays by MoS_2 nanoparticles (Eq. 4):

$$I(s) \sim \exp(-\tfrac{1}{3}R_g^2 s^2), \qquad (4)$$

where R_g is a radius of inertia of the nanoparticles.

In the (s_1, s_2) range power law decline of the intensity is observed $I(s) \sim s^{-n}$, with $n \approx 4.0$. This result indicates the scattering by nanoparticles surface formed of carbon (graphene) layers. The value of $n \approx 4.0$ indicates the implementation of Porod's law of scattering by smooth (nonfractal) surface.

The (s_2, s_{max}) range corresponds to scattering by polydisperse system of mesopores.

On the distribution function of scattering centers there is a broad symmetrical peak at $d \approx 52$ nm that corresponds to the most probable diameter of the MoS_2 nanoparticles. Along with it in the range of 0-25 nm there is a number of peaks corresponding to the most probable mesopore diameters. For the sample after annealing the intensity curve of X-ray scattering has not changed (Fig. 5 c), but on the distribution curve of inhomogenities the peaks mentioned above are reduced due to the decrease in the volume fraction of mesopores after annealing.

Fig. 6 shows the frequency dependence of the complex conductivity in logarithmic coordinates for mesoporous carbon before (-▲-) and after (-△-) annealing in Ar atmosphere at $500^{o}C$ for 2 hours, nanocomposite MoS_2/C before (-●-) and after (-○-) annealing in Ar atmosphere at $500^{o}C$ for 2 hours, and commercial MoS_2 (−) received from Merck KGaA, Germany. The curves for all samples, except for commercial MoS_2, can be divided into two areas: the linear frequency independent region, and the second one, where the conductivity increases sharply with frequency increasing.

4. DISCUSSION

Taking into account the geometrical parameters of pellets made of all samples we calculated the value of electrical conductivity by equation 7, which is derived from the following (Eq. 5 and 6) [12] :

$$\rho^* = \rho' - j\rho'', \qquad (5)$$

Where $\rho' = Z'S/d$ i $\rho'' = Z''S/d$, Z' and Z'' are real and imaginary parts of the complex impedance, S and d are cross-sectional area and thickness of the pellets made of the sample, respectively. The complex conductivity is the reciprocal of the complex resistance:

$$\sigma^* = \frac{1}{\rho^*} = \sigma' + j\sigma'', \qquad (6)$$

where $\sigma' = \rho'/M$, $\sigma'' = \rho''/M$, and $M = |Z^*|^2(S/d)^2$, then:

$$\sigma^* = \sqrt{(\sigma')^2 + (\sigma'')^2}, \qquad (7)$$

Conductivity of mesoporous carbon for the direct current approximation is 0.11 mS/m before and 0.18 mS/m after annealing in argon atmosphere. Such low conductivity of mesoporous carbon is due to a large number of pores and greatly depends on the graphitization degree [13]. At relatively low temperature of carbonization (below 600°C) organic base feedstock is burnt partially and a complex framework of condensed aromatic layers formed by carbon atoms is incomplete. As a result the impedance of the aggregated carbon particles, which depends on the electrical resistance of each particle and the contact resistance between them, remains quite high. Also, the presence of oxygen on nanoparticles surface affects the electrical resistance. According to [14] oxygen-containing compounds that are formed mainly at the edges of graphite fragments, enlarge the barrier for electron transfer from one crystal element to another. In addition, the electrical properties of carbon materials are directly related to their electronic and atomic structures. Typical values of elecrtical conductivity of amorphous carbon is in the range of 10^{-4} [15, 16] as a result of low ohmic contact between particles and carbon graphitization degree. The annealing leads to sintering and tightness of the particles that improved contact between them.

The conductivity of molybdenum disulfide, which refers to semiconductors, according to

published data, at room temperature along the c axis, i.e. perpendicular to the layers, is about 10.4 mS·m^{-1} [17], but for pressed pellets this value is smaller and lies in the range of $10^{-2} - 10^{-4}$ mS·m^{-1} [18, 19]. We measured the conductivity of commercial MoS$_2$ (Merck KGaA, Germany) with an average particle size of 10 μm and it is equal to 0.038 mS·m^{-1}. The conductivity of the synthesized MoS$_2$/C nanocomposite is 0.48 mS·m^{-1} before and 0.51 mS·m^{-1} after the heat treatment in argon atmosphere at the temperature of 500°C for 2 hours (Fig. 6). The conductivity of nanocomposite increased by 3 times in comparison with carbon is due to a synergistic effect of these two materials, in particular carbon acts as a donor of electrons for molybdenum disulfide, which at low frequencies and room temperature is usually *n*-type semiconductor with hopping conductivity, i.e. the exchange of electrons between Mo ions. The excess electrons from the electron donor would be expected to reduce the hardness of the electron transfer and according to Koroteev [20] in the partial electron transfer from graphene (or carbon layer) to MoS$_2$ layers each carbon atom donates ca. 0.027e to MoS$_2$ and the transferred electrons are located on sulfur atoms.

Obtained dispersion curves of dependence of conductivity on frequency ω of applied field (Fig. 6) were approximated by Jonscher's power law in disordered materials (Eq. 8) [21]:

$$\sigma(\omega) = \sigma_{dc} + A\omega^{n}, \qquad (8)$$

where σ_{dc} is frequency independent part of conductivity, A is a temperature dependent constant that gives the information about the strength of the polarizability (or non-ideal conductivity) which comes from the diffusive motion of carriers in the sample. The exponent *n* is the slope of the linear section of the high-frequency dispersion (its value ranges from 0 to 1) and describes the process of charge transfer in disordered materials and is a measure of the interaction between charged particles involved in the processes of polarization and conductivity, and also depends on the temperature. The calculated values of A and *n* are presented in Table 1. For today the universal and exact relationship between these constants is not defined yet, a lot of researches tried to determine it empirically but still not a one assumption was proved. In our case the sample with the lowest *n* has the biggest A value. As to exponent *n*, Jonscher [21] suggested that the range of $0 < n < 0.4$ corresponds to material conductivity based on the existence of conducting grains separated by less conducting barriers. At low frequencies, each grain behaves as a macroscopic

dipole, owing to the migration of a possible negative charge on its surface, which interacts strongly with its neighbors, giving rise to a strong dispersion. As the frequency is increased, this dipole has insufficient time to respond, and the bulk response of the grains predominates [22]. While the range of the exponent $0.4 < n < 0.6$ suggests multipolaron hopping of charge carriers across the interfaces of grains and grain boundaries or at the layers interfaces. This indicated the localized nature of the electronic charge carriers about the ionic sites of the crystal structure [23]. Thus, the annealing in inert atmosphere leads to the differences in the electric conductivity character as a result of microstructural changes in the nanocomposite material.

5. CONCLUSIONS.

Summing up all presented results, the conductivity of synthesized MoS_2/C nanocomposite, which was obtained by direct current approximation, is thirteen times higher than of the commercial MoS_2 with average particle size of 10 μm. The resulted high conductivity of the nanocomposite does not contradict the general patterns of nanoparticles conductivity, which is usually less than of microparticles due to the properties of the large specific surface at which the scattering occurs, and is explained by a synergistic effect between MoS_2 and carbon. This result is important for use in electrochemical electric energy generation and storage devices, especially at its initial designing and elaboration stage.

REFERENCES

[1]   H. Li and Z. Haoshen. Chem. Commun. **48** (9), 1201 (2012).

[2]   H. Li, W. Li, L. Ma, W. Chen, and J. Wang. J. Alloy Compd. **471**, 442 (2009).

[3]   S. Ding, D. Zhang, J. Chen, and X. Lou. Nanoscale **4**(1), 95 (2012).

[4]   S.P. Vattikuti, C. Byon et al (2015) Co-precipitation synthesis and characterization of faceted MoS_2 nanorods with controllable morphologies, Appl Phys A 119(3): 813-823.

[5]   Mak K, Lee C et al (2010) Atomically thin MoS_2: a new direct-gap semiconductor, Phys Rev Lett 105(13): 136805.

[6]   K. Chang, W. Chen et al. J. Mater. Chem. **21**(17), 6251 (2011).

[7]   C. Zhu, X. Mu et al. Angew. Chem. Int. Edit. **53**(8), 2152 (2014).

[8]   N. Li, Y. Chai et al. Mater. Lett. **66**(1), 236 (2012).

[9]   M.A. Lukowski, A.S. Daniel et al. J. Am. Chem. Soc. **135**(28), 10274 (2013).

[10] L. Ma, G. Huang et al. J. Power Sources **264**, 262 (2014).

[11] D.I. Svergun, P.V. Konarev et al. J. Appl. Crystallogr. **36**(5), 1277 (2003).

[12] M. Abdullah and A. Yusoff. J. Alloy Compd. **233**, 129 (1996).

[13] B. Rachiy, B. Ostafiychuk et al. Phys. Chem. Solid State **14**(4), 734 (2013).

[14] S. Biniak, A. Swiatkowski, and M. Pakula. Chemistry and physics of carbon. Marcel Dekker, New York, 2001.

[15] J. Robertson. Adv. Phys. **35**(4), 317 (1986).

[16] C. Godet. Philos. Mag. B. **81**(2), 205 (2001).

[17] S. Guha Thakurta and A. Duttai. J. Phys. Chem. Solids **4**(5), 407 (1983).

[18] E. Benavente, M. Santa Ana, and G. Gonzalez. Phys. Status Solidi B **241**(10), 2444 (2004).

[19] M. Ahmad, M. Rafiq et al. J. Appl. Phys. **114**(4), 043710 (2013).

[20] V. Koroteev, L. Bulusheva et al. J. Phys. Chem. **115**(43), 21199 (2011).

[21] A. Jonscher. J. Non-Cryst. Solids **8**(10), 293 (1972).

[22] A. Fourrier-Lamer, A. Fizazi, and N. Belhadj-Tahar. Synthetic Mets. **24**, 95 (1988).

[23] R. Bhrowmik and N. Naresh. J. Phys. Chem. Solids **73**(2), 330 (2012).

[24] Z. Wang, T. Chen et al. J. Mater. Chem. A. **1**(6), 2202 (2013).

Table 1 The data obtained from Jonscher's power law approximation

Sample	A	n	σ_{dc}, mS·m^{-1}
C	$5.4 \cdot 10^{-6}$	0.42	0.11
C (500°C, Ar)	$7.6 \cdot 10^{-6}$	0.42	0.18
MoS$_2$/C	$2.0 \cdot 10^{-5}$	0.34	0.48
MoS$_2$/C (500°C, Ar)	$2.7 \cdot 10^{-6}$	0.47	0.51

Fig.1 Diffraction patterns of obtained materials after heat treatment at 80°C (a), 500°C (b)

Fig. 2 TEM images of the material obtained by hydrothermal synthesis after heat treatment at 500°C

Fig.3 The atomic content of components C, Mo, S and O in a fragment of the synthesized composite along the line of 2 μm by EDS
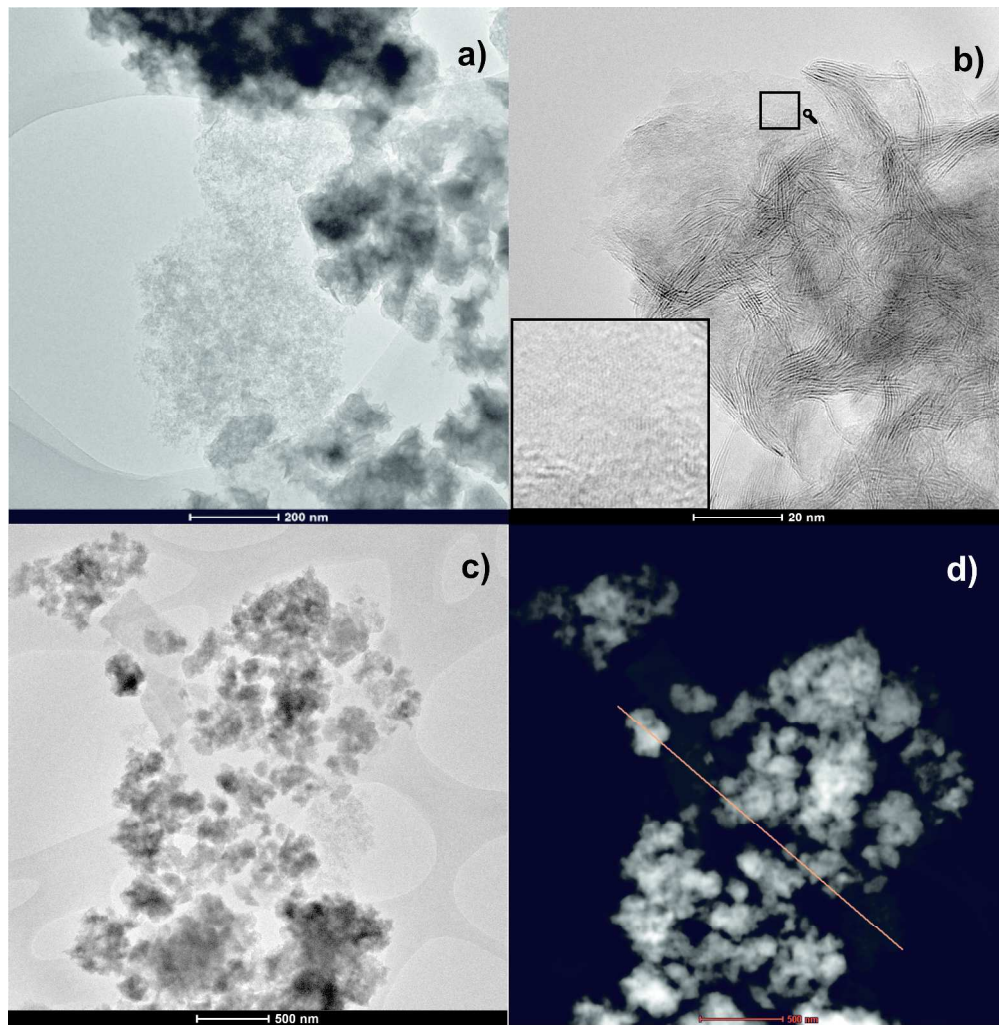
Fig. 4 Pore size distributions for C (black bar) and MoS$_2$/C (gray bar)

Fig. 5 The curves of scattering intensity of X-rays at small angles (a, c) and calculated scattering centers distribution function (b, d) for the material samples annealed at 80°C and 500°C, respectively
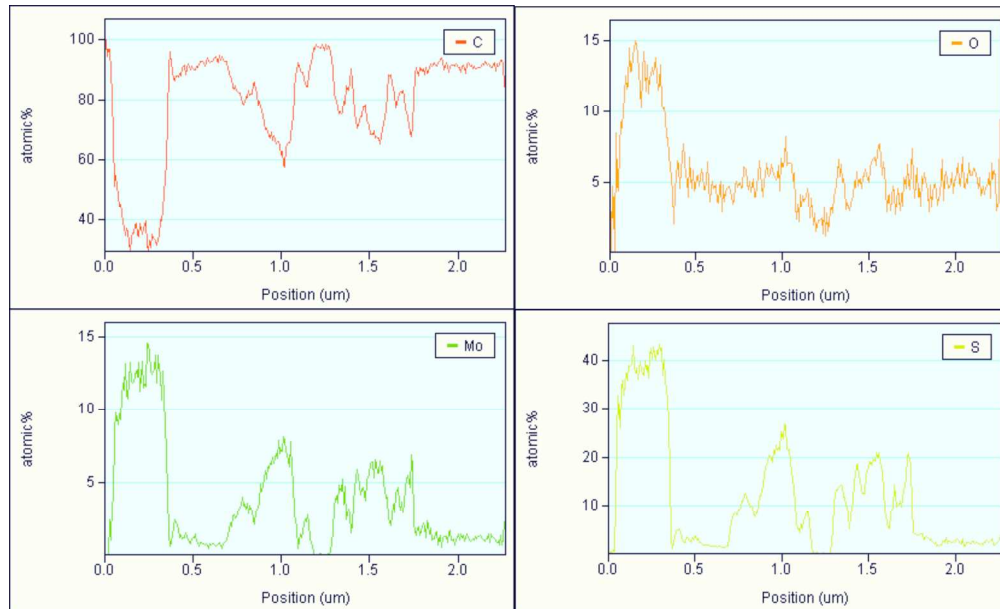
Fig. 6 Frequency dependent electrical conductivity of the samples.
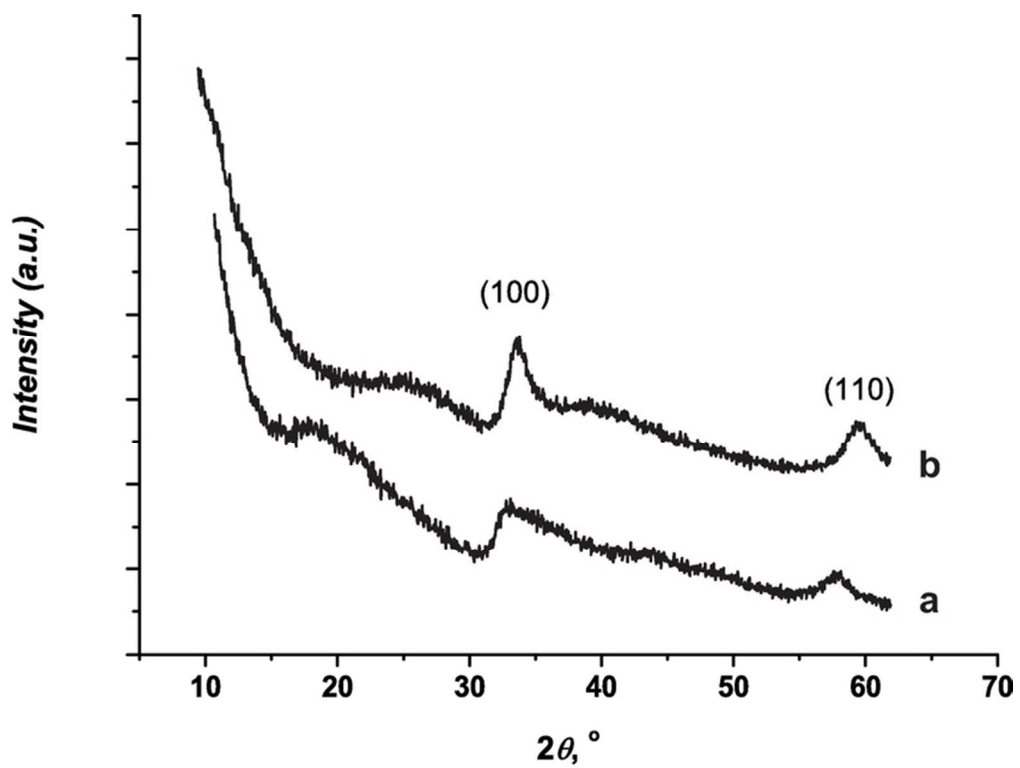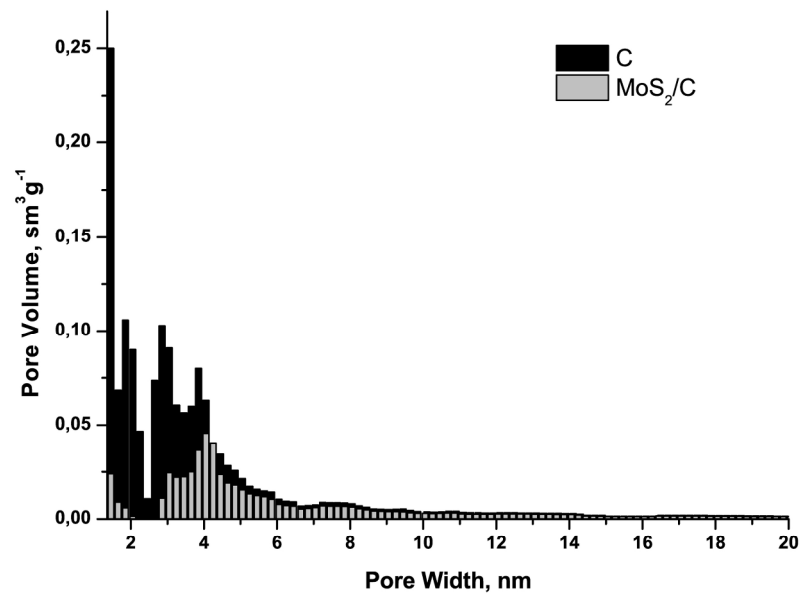
Diffraction patterns of obtained materials after heat treatment at 80°C (a), 500°C (b)
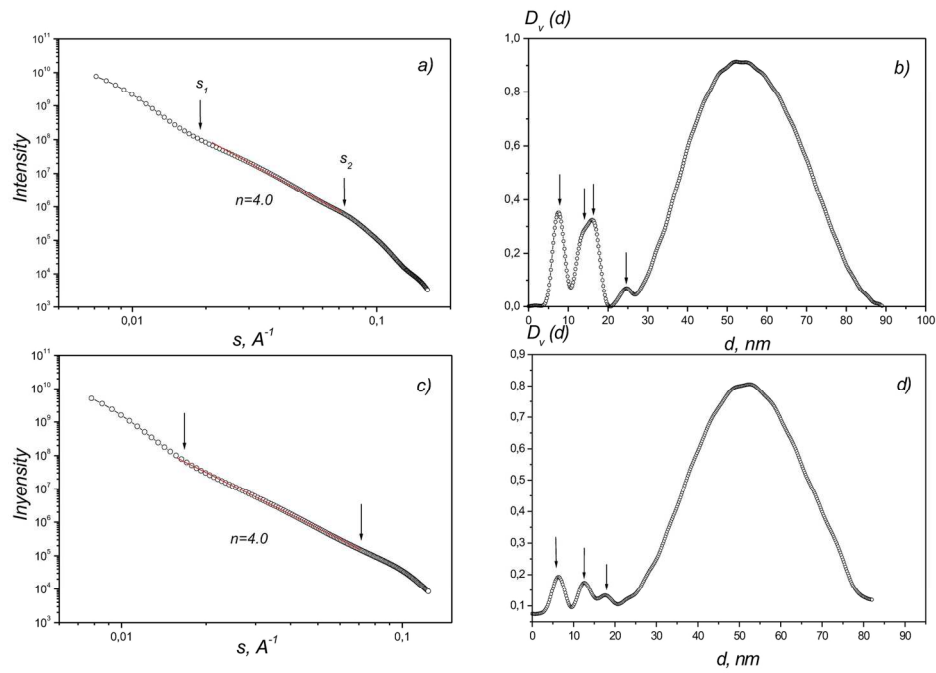70x53mm (300 x 300 DPI)

TEM images of the material obtained by hydrothermal synthesis after heat treatment at 500°C
373x379mm (300 x 300 DPI)

The atomic content of components C, Mo, S and O in a fragment of the synthesized composite along the line of 2 μm by EDS
292x177mm (300 x 300 DPI)

Pore size distributions for C (black bar) and MoS_2/C (gray bar)
209x148mm (300 x 300 DPI)

The curves of scattering intensity of X-rays at small angles (a, c) and calculated scattering centers distribution function (b, d) for the material samples annealed at 80°C and 500°C, respectively
155x107mm (300 x 300 DPI)
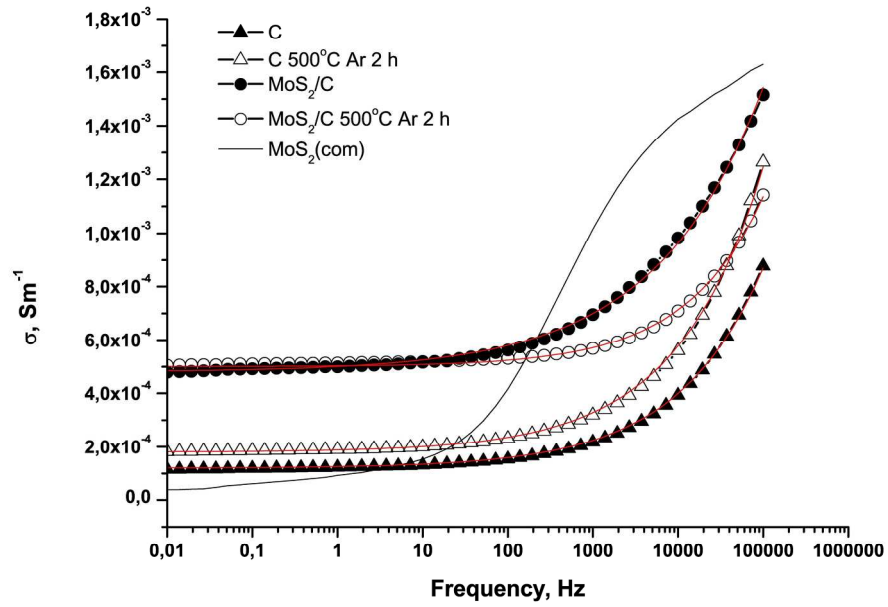
Frequency dependent electrical conductivity of the samples.
209x148mm (300 x 300 DPI)